Performance of a Low-Density Hypersonic Magneto-Aerodynamic Facility

R. Kimmel, J. Hayes, C. Tyler
Air Vehicles Directorate, Air Force Research Laboratory
Wright-Patterson AFB, OH

J. S. Shang
Department of Mechanical and Material Engineering, Wright State University
Dayton, OH 45435

Abstract

A hypersonic, weakly ionized gas experimental facility has been successfully developed for magnetoaerodynamics basic research. The weakly ionized air is generated by a combination of direct current discharge, radio frequency discharge, and a combination of both in a blow-down, open jet, Mach 5 flow channel. The plasma field is characterized by electron temperatures around 10,000 K, and electron number density up to $2x10^{12}$ cm^{-3}. The magnetic field is provided by a steady sate solenoid that can generate a maximum field up to three Tesla and an array of permanent magnets. In this environment, the maximum magneto-aerodynamic interaction parameter per unit length is around 1.5 per meter. A collection of plasma diagnostic tools including emission spectroscopy, microwave absorption, and Langmuir probes also are available.

Introduction

There is little doubt that electromagnetic-aerodynamic interaction adds a new physical dimension to aerospace vehicle performance. In particular, the Lorentz force and Joule heating introduce new mechanisms that couple directly between kinetic, thermal, and electromagnetic energy to create numerous technical possibilities for aerodynamic performance enhancement.[i] However, this added physical dimension is realizable only in an electrically conducting medium and in the presence of applied and induced electromagnetic fields. In hypersonic flight, the thermal excitation associated with bow shock compression can ionize air in a shock layer to create the desired flow

Report Documentation Page

Form Approved
OMB No. 0704-0188

1. REPORT DATE	2. REPORT TYPE	3. DATES COVERED
20 OCT 2003	**N/A**	**-**

4. TITLE AND SUBTITLE	5a. CONTRACT NUMBER
Performance of a Low-Density Hypersonic Magneto-Aerodynamic Facility	5b. GRANT NUMBER
	5c. PROGRAM ELEMENT NUMBER
6. AUTHOR(S)	5d. PROJECT NUMBER
	5e. TASK NUMBER
	5f. WORK UNIT NUMBER
7. PERFORMING ORGANIZATION NAME(S) AND ADDRESS(ES) **Air Vehicles Directorate, Air Force Research Laboratory Wright-Patterson AFB, OH; Department of Mechanical and Material Engineering, Wright State University Dayton, OH 45435**	8. PERFORMING ORGANIZATION REPORT NUMBER
9. SPONSORING/MONITORING AGENCY NAME(S) AND ADDRESS(ES)	10. SPONSOR/MONITOR'S ACRONYM(S)
	11. SPONSOR/MONITOR'S REPORT NUMBER(S)

12. DISTRIBUTION/AVAILABILITY STATEMENT
Approved for public release, distribution unlimited

13. SUPPLEMENTARY NOTES
See also ADM001739, Thermochemical processes in plasma aerodynamics (Conference Proceedings, 28-31 July 2003 (CSP 03-5031)., The original document contains color images.

14. ABSTRACT

15. SUBJECT TERMS

16. SECURITY CLASSIFICATION OF:			17. LIMITATION OF ABSTRACT	18. NUMBER OF PAGES	19a. NAME OF RESPONSIBLE PERSON
a. REPORT **unclassified**	b. ABSTRACT **unclassified**	c. THIS PAGE **unclassified**	**UU**	**20**	

medium. The plasma is generated at high temperatures difficult to sustain in a ground testing facility. Any meaningful ground simulation therefore must rely on similitude.

To simulate strong hypersonic magneto-aerodynamic interaction in a ground facility requires an environment where the plasma interaction parameter, $\sigma B^2 L / \rho U$, approaches or exceeds unity. This requirement is particularly severe for a weakly ionized gas generated by valence discharge in a laboratory environment. The ionization process frees only outer shell electrons and occurs at the Stoletow point. For air the energy addition is about 81 eV per ion-electron pair.[ii,iii] The ionization process by valence discharge is energy efficient but also has a relatively low upper limit in electron number density. From prior experience using direct current (DC) discharge, radio frequency (RF) discharge, and electron beam, the value is generally up to 10^{13} cm^{-3} and the electron temperature is in the range of 10,000 K.[iv,v,vi] Under these conditions, the electric conductivity of the plasma is around 10 mho/meter, an order of magnitude lower than the typical space vehicle reentry condition. This shortfall therefore must be compensated by the other pertaining variables of the plasma interaction parameter – the magnetic flux and air density.

For most aerodynamic applications, the typical magnetic Reynolds number is much less than unity, which implies the induced field is negligible in comparison with the applied field. The applied electromagnetic field therefore will dictate the magnetoaerodynamic interaction. Examination of the magnetoaerodynamic interaction parameter shows that dynamic similitude can be manipulated most effectively through the applied magnetic field intensity. The magnetic field generated either by a solenoid or permanent magnet behaves similarly to a dipole. The intensity decay is faster than the inverse cubic power to the distance from the magnetic pole. The increased intensity in the interactive field can be achieved by increasing the magnetic field strength, and by shortening the gap between magnetic poles. Meanwhile the test section should also have a suitable dimension to allow a uniform and unperturbed stream. Reducing the physical dimension of the test section while still maintaining an inviscid core for aerodynamic evaluation can meet the latter requirement. The reduced length scale arising from the smaller model size must be compensated for by lowering the density of the wind tunnel.

Finally and not the least, all efforts must be exercised to raise the electron number density as high as possible. From the foregoing discussions, the present effort is focused on the trade-off of key variables to obtain the maximum plasma interaction parameter by a low-density hypersonic plasma tunnel.

Increasing magnetic field strength in the test section and electrical conductivity of the air plasma become the principal concerns for the new facility. In order to increase magnetic field strength, the distance between the magnet poles is shortened by applying the field across the smaller dimension of a rectangular test section. A pair of solenoids capable of generating up to three Tesla is placed outside the test chamber to sustain a uniform magnetic field. By a combined application of DC discharge and RF radiation for plasma generation, the electron number density is anticipated to double its value. Systematic research in electrode size, shape, and placement will also be performed to achieve the optimal condition for strong electromagnetic and aerodynamic interactions.

A computational and experimental approach is necessary to describe the compact flow field structure within the facility. The mass-averaged Navier-Stokes equations are solved to describe the detailed flow field from nozzle settling chamber to the diffuser. Efforts are concentrated on characteristics of the boundary-layer on the tunnel walls and the free-shear layer shedding from the nozzle into the test chamber. This information is used for electrode placement and for determining the hypersonic inviscid core size. All data will be validated by redundant measurements or comparing with calculations whenever possible.

Experimental Facility

The hypersonic low-density tunnel is a basic, blow-down, free-jet facility. The rectangular cross-section, conical nozzle with a throat area of 73.7 x 5.08 mm expands to a nozzle exit plane of 73.7 x 177.8 mm. It is designed to deliver a nominal Mach 5 flow in the test section. The test section currently in use has dimensions of 386.08 x 177.8 x 73.66 mm (LxHxW). The diffuser is designed to achieve at least normal shock recovery and the entire length of the tunnel is 1555 mm. To avoid unintentional grounding the experimental facility is constructed of Plexiglas.™[vii] For non-intrusive diagnostic

measurements, two 235 mm diameter quartz windows were mounted on the side walls of the test section. The window exposes the entire test section including the nozzle exit plane. A sketch of this plasma channel is presented in Figure1. Dry air is supplied from the facility bottle farm through a three-stage pressure-reduction system. The tunnel exhausts to a 2800 m^3 vacuum sphere.

The simulated altitude range (based on static density) of the new facility extends from 30,000 to 50,000 meters (100,000 to 150,000 ft). At a fixed stagnation temperature of 300K, the tunnel has an operational stagnation pressure range from 0.1 to 1.0 atmosphere, and in this pressure range the air stream is free from condensation. At a stagnation pressure of 300 Torr, the free-stream in the test section has a velocity, density, and temperature of 698.4 m/s, 0.005 kg/m^3, and 51.6K, respectively. Under these conditions the mass-flow rate is 0.046 kg/s and the unit Reynolds number in the test section is $1.15x10^6$ per meter.

The relatively shorter span between the tunnel sidewalls than the vertical walls is designed to achieve the maximum transverse magnetic field strength with the narrowest gap between the poles of magnets. Meanwhile this construction also must maintain an inviscid core in the test section. From the basic rectangular nozzle and diffuser configurations, the available uniform flow field for testing is confined within a rhombohedron. The maximum testing cross-section is estimated to be 38x105 mm immediately downstream of the nozzle exit. This physical dimension also limits the size of model that can be tested before blockage significantly alters the characteristics of the flow field.

Another unique feature of the Mach 5 tunnel is the low density environment. To achieve a strong magnetoaerodyanmic interaction, the plasma channel is operated at stagnation pressures ranging from 0.1 to 1.0 atmosphere. Under these conditions, the air density in the inviscid core spans a range from 0.0013 to 0.013 kg/m^3, and the neutral particle number density ranges from $3x10^{16}$ to $3x10^{17}$ cm^{-3}. As a consequence mass flow rates vary from 0.007 to 0.13 kg/s, and continuous operation can be easily sustained.

A three-dimensional traverse mechanism has also been developed for the facility as a part of the data gathering and reduction process. This mechanism has a freedom of

movement to cover the entire domain of the test section (152 x 74 x 178mm). The placement of the traverse is controllable within a distance of 0.25 mm. For flow visualization, a single-pass schlieren system with an arc lamp light source and a high-speed video camera were used. All experimental data were collected with an HP 3852A data acquisition and control systems.

Plasma Generation

The air plasma in the present hypersonic channel is generated by either DC discharge, RF radiation, or a combination of both. In previous efforts to measure plasma properties in a vacuum chamber, the impedance of DC discharge has been reduced by a factor near two at the Stoletow point by adding RF radiation to plasma.[viii] RF radiation was effective in enhancing the DC discharge in a vacuum chamber even at a static pressure as high as 7 Torr. In the test section of the channel, the energy balance between the vibration-translation energy pumping and the inelastic collision with neutral heavy particles is much more complex.[ii,vi] To overcome the principal loss from attachment processes, both from the ground state and metastable molecules, the DC and RF discharges are operated simultaneously to increase the charged particle density.

The electrode arrangement for the best concentration of charged particles upstream of a model is to adopt the model as the cathode and place the anode external to the free jet stream. Unfortunately this setup is not always possible, because of the large disparity in density between the inviscid core and the free shear layer. The lower electrical resistance in the shear layer encourages a discharge path through the shear layer and the wake region of the model. To remedy this behavior, the distance between electrodes must be shortened and the electrodes exposed to the on-coming stream. An undesirable attribute of this electrode arrangement reduces the unperturbed freestream available for experiments.

The DC discharge is provided by a group of Universal Voltronics reversible polarity switching power units. One of the units is rated at 8 kW with 10kV output source at a signal impedance of 10^4 Ohms. At the breakdown voltage of 400V, a diffuse discharge was achieved at a plasma current as high as 550 mA. The discharge changes

into multiple streamers when the electrical current exceeds 900 mA. Other DC power supply units are also available they are rated at 4 kW with 10kV output source at the same impedance. The maximum current output however is limited to 400 mA.

The RF power supply and its automatic matching network are the Dressler CESAR-1350 and VM5000W, respectively. This integrated unit is water-cooled and can deliver up to 5 kW at 13.56 MHz into a 50 Ohm load. In fact, the RF plasma generation is not treated as an antenna problem, but as a RF carrying electrode with an ambient ground plane. In routine operation, the automatic matching network will keep the reflected power to less than two percent. These observations reflect the fact that the RF operating frequency is compatible with the electron neutral collision frequencies from 10 to 100 MHz for maximum energy transfer to an electron. Figure 2 depicts the weakly ionized gas generated by the RF antenna. Although a high concentration of the charged particles was detected in the relatively low density region of the shear layer, the plasma generation process can still be enhanced by the secondary emission in the hypersonic stream.

Applied Magnetic Field

A key element in simulating the magnetoaerodynamic interaction in flight is the strength of the applied magnetic field. Based upon the magnetic interaction parameter, the low electron number density in the ground testing facility must be compensated by the applied magnetic field strength, B. In fact, it is also the most effective control parameter. In the present facility, the transverse magnetic field can be generated by a steady state solenoid and an array of Neodymium rare earth (NdFeB) permanent magnets.

The principal electromagnet system is the GMW 3474 water cooled model with a pole cap diameter of 250 mm. The coils, when connected in series, have the maximum resistance of 0.54 ohms, a self-inductance of 80 mHenries, and a maximum power rating of 10.6 kW (140 amp, 76 Volts). At the pole gap of 10mm and the pole diameter of 25 mm, the field strength is as high as 3.5 Tesla. The field strength diminishes drastically as the pole gap increases. The pole diameter may be increased to generate a larger uniform magnetic field, but this comes at the expense of reduced field strength. In the present facility, the gap dimension is determined by the tunnel span and sidewall thickness for a total of 139.7 mm. Under these conditions, the transverse magnetic field has a magnitude of one Tesla and is nearly uniform.

Based upon the known applied magnetic field strength and the electrical conductivity of the generated air plasma, the magnetoaerodynamic interaction parameter per unit length in the present facility is estimated around 1.5. This value is based upon a conductivity, σ, of 10 mho/m.

Diagnostic Capability

A critical element of the present effort is the development of diagnostic capability for determining the properties of a weakly ionized gas. Several parameters are important in magneto-aerodynamics. One group is the temperatures of various internal-degree-of-freedom – the translation, rotation, vibration, and electron excitations. These data describe the distribution of possible species concentration and the energy state of the gas mixtures. The other group of parameters includes the electrical conductivity, electron, and ion number density. These data are the intrinsic properties of the plasma medium. A combination of direct and non-intrusive techniques are used to measure them.

A system for rotational and vibrational temperature measurement using emission spectroscopy was acquired from Research Support Instruments, Inc. The system hardware consists of a fiber-optic probe connected to an Ocean Optics PC 2000 spectrometer. A collimating head may be attached to the fiber-optic probe to improve spatial resolution. Software is provided to drive the spectrometer and analyze the spectra for vibrational and rotational temperatures using the well-known Boltzman-plot method. The system measures the spectrum of the second positive group of nitrogen ($N_2(C^3\Pi_u) \rightarrow N_2(B^3\Pi_g)$ transition).[ix] The logarithms of relative intensities of transitions are plotted versus wavenumber. A straight line is curve-fitted through these points, and rotational and vibrational temperatures are extracted from the slope of the line. Rotational lines are not fully

resolved by the spectrometer, but rotational temperatures are estimated by convolving the predicted spectrum with the slit function of the spectrometer and comparing it to the measured spectrum. Curve-fitting of the rotational temperature is done in 10K increments, effectively creating a 10K resolution in the measured temperature. Integration times for the spectral measurements described below ranged from 3 msec to 50 sec, depending on the signal strength, but the limiting factor in the data acquisition rate is the time to required for curve-fitting for rotational temperature measurements. Maximum data acquisition rates were several Hz.

DC discharges were generated between two flat plates, 46 mm in length in the streamwise direction and 6mm wide in the spanwise direction. The electrodes were relieved approximately 5 deg to create a low-density region on adjacent surfaces to help guide the discharge between them. Electron temperatures are in the range of 8000 to 14000K

Rotational and vibrational temperatures for a range of discharge currents, measured in the center between the two electrodes are shown in Figs. 3 and 4, respectively. Rotational temperatures at this location range from approximately 70K for the 50 mA discharge to near 200K for the 400 mA discharge. Error bars are represent a 1σ-deviation from the mean, based on multiple measurements, and are thus represent the signal unsteadiness. Unsteadiness as measured by the rms is quite high for discharges above 100 mA, but measurements show a trend of increasing rotational temperature with increasing current. Vibrational temperatures range from about 4000K at 50 mA, and increase up to about 200 mA. Above this current, they appear to saturate at about 5000 to 7000 K.

A sustained development of a double Langmuir probe has been successfully carried out by Menart et al.[x] This probe is constructed of twin 0.2 mm diameter platinum wires embedded in a ceramic sleeve, with a separation distance of 0.5 mm. The sleeve covers all but 1.27 mm from the tip of the wires, thus the sensing area for each wire is merely 0.83 mm^2. A major equipment improvement for this measuring system is the installation of a Magnavolt bi-polar power supply to the Keithly 230 programmable voltage source. The Keithly 230 has 100 programmable channels that have at +/- 100 V range with +/- 100 mA current limitation. This power supply has isolation capabilities of 10,000 Volts to protect the data collecting system from extreme high voltage fluctuations.

A series of Langmuir probe measurements were taken using the DC electrode rods with gap distances of 50 mm and 64 mm. The data depicted in Figures 5 and 6 were collected adjacent to the vertical center line between electrodes and the test section. In general, the electron temperature

measurements agree very well with the data from an optically pumped plasma.[xi] In Figure 5, the measured electron temperatures are presented over the entire discharge current range. At the hypersonic flow condition, the data scatter of the electron temperature is rather large, reflecting the unsteady discharge behavior. Nevertheless the electron temperature of the DC glow discharge generated by electrode rods lies in the range from 10^4 to 10^5K.

The measured ion number density distribution is given in Figure 6. These data were collected with the electrode rod arrangement for discharge currents up to 500 mA. Again, rather large data scatter is apparent. An average value over the entire measured range is around $2x10^{12}$ cm^{-3}. From the measurements, the mean-free-paths of the electrons and ions are determined to be around 150 and 30μm respectively. The Debye length is about 70 μm. These characteristic lengths associated with the probe put the measuring environment in the transitional regime.[xii,xiii] However, some of the data repeatability issues are incurred by the rather thin discharge domain between the rod electrodes which will be improved by different electrode shape and plasma generation mechanisms. Another improvement in the data collection process will be concentrated on keeping the probe contamination to an absolute minimum.

The most recent and non-intrusive plasma diagnostics for the Mach 5 Plasma channel is based on the dispersive property of a microwave that propagates in plasma.[xiv] The operational principle is that when the incident microwave has a higher frequency than the plasma frequency, $\omega_p = \sqrt{ne^2/\varepsilon_0 m}$, the microwave will attenuate and exhibit a phase shift. The basic measuring system consists of a Roscoe Microwave generator with a detector, an HP 5340 Microwave frequency counter, and two sets horn antennae. The microwave generator has a frequency range from 10 to 18 GHz, at a maximum output of 14.9 dbm (31mW). The detector has a sensing upper limit of –25 dbm (0.034 mW). This system therefore can measure an electron number density up to about 10^{13} cm^{-3}, and has the spatial resolution of 42 mm. A series of tests was carried out to determine the peak power obtainable at different separation distances between transmitting and receiving horns. Progress has also been made to establish a preferred procedure for data collection, including the use of absorbing material in the beam path to suppress standing waves between the two horns at higher frequencies. A detailed description of all plasma diagnostic tools for the Mach 5 channel can be found in the two papers by Menart et al.[xii,xiii]

In the present effort, the determination of the electrical conductivity and plasma temperature is most challenging. The Langmuir probe is a very robust means for measuring the electron number density

and electron temperature in plasma.[vi,xii] However, the data reduction process is often very demanding, especially when the testing environment is far from ideal for Langmuir probe operation, such as a flow field in the transitional region between the collisionless and continuum domains and in the hypersonic stream. Meanwhile the plasma field also contains high gradient regions. It is believed that the charged particle number density can be measured within a factor of three in the tested range (10^{12} cm^{-3}). The greatest uncertainty in these results comes from flow field interference to the data collecting process. This result reflects the current state-of-the-art of Langmuir probes in determining transport properties of plasma in hypersonic stream.

Numerical Analysis

In order to verify the design flow field characteristics and provide a detailed electrode placement analysis, a numerical analysis for the complete Mach 5 channel was performed. The numerical simulation needs to describe the flow field starting from the nozzle throat until far downstream of the diffuser. The diffuser is designed for a normal shock recovery, thus a strong shock-wave boundary-layer interaction is anticipated in the computational domain. The numerical simulation is obtained by solving the mass-averaged, time dependent, three-dimensional Navier-Stokes equations. This system of equations is solved by an implicit, time accurate, unstructured Euler/Navier-Stokes solver, Cobalt.[xv] The numerical algorithm is based on the Riemann formulation of Gottlieb and Groth[xvi] and implicit time stepping to yield second-order spatial and temporal accuracy. The second-order spatial accuracy is achieved by the least-squares total variation diminishing scheme in the flux reconstruction process. The viscous flux vectors are formulated to satisfy the discrete maximum principle that guarantees conservation and yields a linearity preserving discretization. The neighbor-cell connectivity of an unstructured grid formulation greatly enhances an exceptional scalable, parallel computing performance when this numerical procedure is ported to multi-computers using a Message Passing Interface (MPI) library.[xvii]

The mass-averaged Navier-Stokes equations in integral form are written as follows:

$$\frac{\partial}{\partial t}\iiint U dv + \iint \left(F_x^+ + F_x^- + G_r^+ + G_r^-\right)\cdot \bar{n} ds + \iint \left(F_{x,v} + G_{r,v}\right)\cdot \bar{n} dx = 0$$ where $F_x^+, F_x^-, G_r^+, G_r^-$ are the split flux vectors derived from the inviscid terms. $F_{x,v}$ and $G_{r,v}$ are the flux vectors of the viscous terms in the governing equations.

The governing equations are discretized by the fully implicit numerical scheme as:

$\left[3\left(U^{n+1} - U^n\right) - \left(U^n - U^{n-1}\right)\right]/2\Delta t + \nabla \cdot F = 0$ where the U's are the conservative independent variables U(ρ, ρu, ρv, p). The reconstruction of the flux vectors at the centroid of the cell faces is by a least-square solution to the following approximation:

$$U_{i\pm 1/2} = U_i \pm \bar{r}\cdot \nabla U_i$$

where the $U_{i\pm 1/2}$ are the reconstructed left and right-side of the variables at the cell interface and ∇U_i is the gradient vector for the cell i.

In the present application, the no-slip velocity components and the constant temperature condition are imposed on the flow channel walls. The surface density value is then obtained by the zero normal pressure gradient approximation. The sonic throat condition is specified at the upstream boundary, and the no-reflection condition and a prescribed reservoir pressures are used at the far downstream of the diffuser. Turbulent closure is achieved by the Spalart-Allmaras one-equation model.[1]

The entire flow field of the Mach 5 Channel is simulated by a three-dimensional mesh system of 1,665,104 cells. At any given streamwise cross section, the flow field is resolved by no less than 8,000 cells. The finest cell spacing adjacent to the solid surface is maintained in the law-of-the-wall variable to the order of magnitude of unity, $2.08 \le y^+ \le 3.24$. The numerical result is obtained for the stagnation pressure of 300 Torr and stagnation temperature of 300 K respectively. To ensure a stable and converged numerical result, the far downstream pressure is set to be lower than the vacuum sphere, 2.5 versus 8 Torr.

---

[1] Spalart, P. R., and Allmaras, S. R., "A One-Equation Turbulent Model for Aerodynamic Flows," AIAA 92-0439, January 1992.

The numerical result verifies the design condition, indeed a Mach number of 5.09 inviscid core is achieved at the nozzle exit. The flow is continually expanded down stream and reaches a maximum Mach number of 5.27 at a distance 102 mm farther downstream. From the numerical simulation, the boundary layer thickness on the channel side wall is determined to be 12 mm, so the useable inviscid core at the nozzle exit is around 50 mm. All this detailed flow field structure can be discerned in Figure 7, a closeup side view of computed density contours. The most predominant feature is the coalescing shock waves in the test section that originated at the trailing edge of the nozzle. These shock waves are further reinforced by the diffuser downstream. The available rhomboidal uniform inviscid core can be slightly enlarged by a higher stagnation pressure condition.

Flow Field Survey

At the present low-density freestream condition, a high resolution schlieren image faces severe technical challenges. For the present purpose, the flow field structure is determined by a Pitot probe survey. All data were collected with a single pressure transducer. The Baratron MIS model 722-A-23320 absolute pressure gauge has a calibrated accuracy of +/1 0.1% of the 100 Torr full range. The flow field structure in the test section is described by traversing the probe at three streamwise locations, the nozzle exit plane, 50.8 mm, and 101.6 mm downstream. In the present effort, data were collected for two stagnation pressure conditions, 300 and 460 Torr. At each stagnation pressure, three sets of survey data were collected in the center plane along the z coordinate and one set of data along the y coordinate across the half span. Accompanying numerical simulation however, is limited to the lower stagnation pressure condition. Additional and more detailed surveys are underway.

Figure 8 presents Mach number profiles on the channel centerline at the nozzle exit plane. These Mach number profiles are deduced from the Rayleigh Pitot pressure formula at different vertical locations. These data were collected at a stagnation temperature of 300 K and stagnation pressures of 300 and 460 Torr respectively. Under these conditions the inviscid core has a dimension more than 107 mm in the z coordinate irrespective of the different stagnation pressures. At the lower stagnation pressure the deduced Mach profile has an average value of 5.14. At the higher stagnation pressure, the core Mach number is approximately 5.22. These data are in good agreement with the numerical result both in the Mach number (5.09) and core size.

The Mach number profiles at a distance of 50.8 mm downstream from the nozzle exit plane are depicted in Figure 9. At this location, the computed Mach distribution is bracketed by the data from two different stagnation pressure conditions. The Mach number data exhibit a scatter from 5.03 to 5.23, and the computed result shows a value of 5.19. Equally important, the measured and computed inviscid core also reach a good agreement.

The last survey station at a distance of 101.6 mm downstream of the nozzle exit plane is shown in Figure 10. At this survey station, the computed result is again bracketed by the measured Mach numbers, with vsalue from 5.12 to 5.28. The higher measured data are generated at the higher stagnation pressure condition. The numerical result indicates a value of 5.27 in the inviscid core along the vertical or the z coordinate. For the present purpose, the comparison between experiment and computation ensures that a sizable unperturbed inviscid core is available.

Numerical results show that axial gradients in the flow are essentially negligible in the test section. On the centerline of the channel, the Mach number changes from 5.09 at the nozzle exit plane, to 5.19 at a distance of 50.8 mm, and 5.28 at the farthest survey station downstream. The centerline Mach number varies by less than a value of 0.18 over the measurement region, or less than 3 percent. This aerodynamic quality is remarkable for a channel of this small dimension.

Figure 11 depicts the transverse Pitot pressure surveys in the test section. Two sets of data at stagnation pressures of 300 and 470 Torr were collected at the nozzle exit plane and across the half span of the channel. In the range of Reynolds number tested, both data sets indicate a sidewall boundary layer thickness about 7 mm beneath a weak shock. Three computed Mach number profiles are included in this figure, corresponding to the identical survey stations in the vertical (z coordinate) direction. Results for the two downstream stations plotted in shifted ordinates for clarity.

The overall survey data reveal a uniform 100x50 mm inviscid core extending a distance of 200 mm from the nozzle exit plane downstream. Although the core size of the low-density tunnel is rather limited, the flow quality in terms of low streamwise gradient is excellent.

In spite of the fact that the plasma is in a thermodynamic non-equilibrium state, the chemically reacting phenomenon of the present analysis is considered negligible. The employed ionization process acts mostly on the outer shell of electrons, the so-called valence electrons. The transfer of kinetic energy to heavy neutral particles is small, therefore, the air temperature in general bears no relation to electron energy.[ii,iii,iv] However, it is not certain this observation is pertinent to the present

facility. First, the energy input for the present facility is extremely limited. A typical value of 10 kW is required to sustain this operation. Second, the combined energy input of the RF radiation and DC discharge is significant to exceed 2kW or more. Lastly, the electrode placement is far upstream of the test section to allow ample inelastic collisions for the energy transferring process. For these reasons, additional flow field surveys will be performed to assess the flow characterstics under different ionization procedures.

Conclusion

A low density plasma channel for basic research has been successfully developed for simulating the flight environment up to 50,000 meters (150,000 ft) at a flight Mach number of 5. A weakly ionized gas generated by DC discharge alone can be characterized by an electron temperature about 10,000 K, an electron temperature about 10,000 K, an electron density up to $2x10^{12}$ cm^{-3}, and an electric conductivity of 2 mho/m. A steady sate solenoid has been integrated into the experimental facility. The experimental data confirm that the electromagnetic-aerodynamic interaction parameter per unit length is around 1.5 per meter.

Significant progress has been made in research for diagnostic tools for determining intrinsic properties of weakly ionized gas including optical spectrometry, microwave devices, and Langmuir probes. Hopefully a set of benchmark experimental data for computational magneto-aerodynamics will be derived from this new facility.

Acknowledgments

The research team is grateful for the vision and leadership of Col. David Walker when he led the Air Vehicles Directorate, Air Force Research Laboratory. This facility would not have come to fruition without his support and encouragement. The sponsorship of Dr. J. Schmisseur of the Air Force Office of Scientific Research is also deeply appreciated. The contributions by Dr. Juan Martinez of the Air Force Research Laboratory, Prof. James Menart and his students Sean Henderson and Andrew Kurpik. The computing resource was supported by the Computational Science center of Excellence, Air Force Research Laboratory at Wright-Patterson Air Force Base.

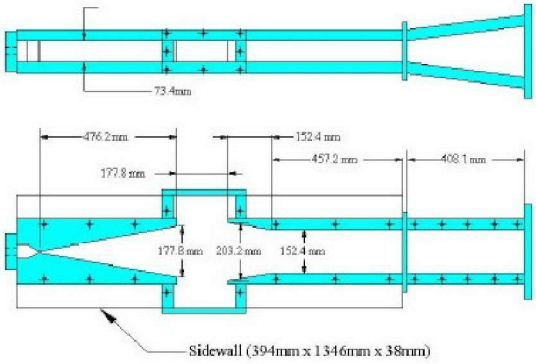

Figure 1 Sketch of the Mach 5 Plasma Channel

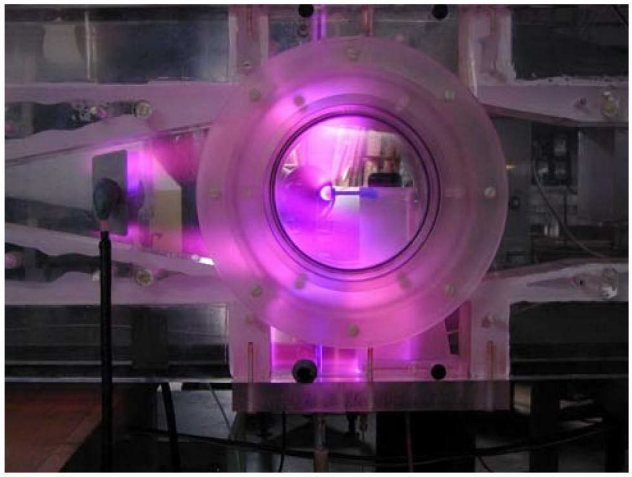

Figure 2 RF discharge in the Plasma Channel

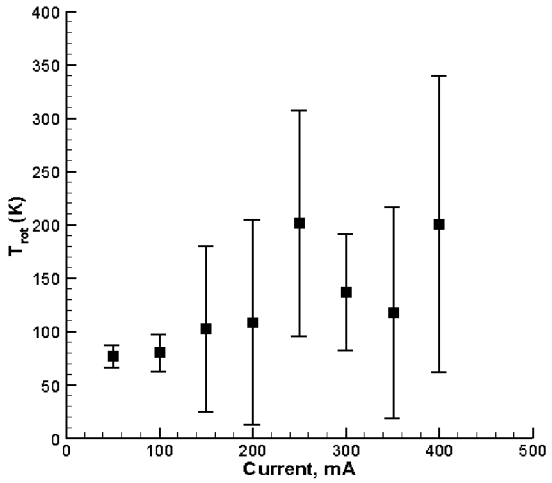

Figure 3 Rotational temperatures via DC discharge

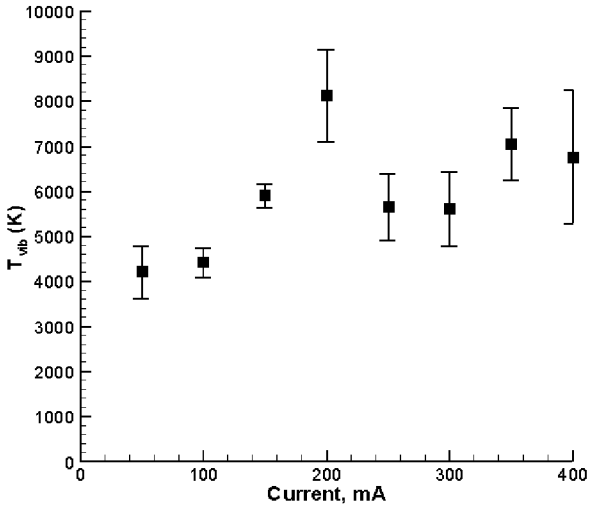

Figure 4 Vibrational Temperatures via DC discharge

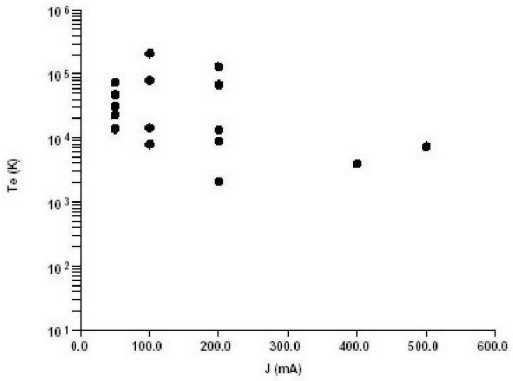

Figure 5 Electron temperature of DC discharge

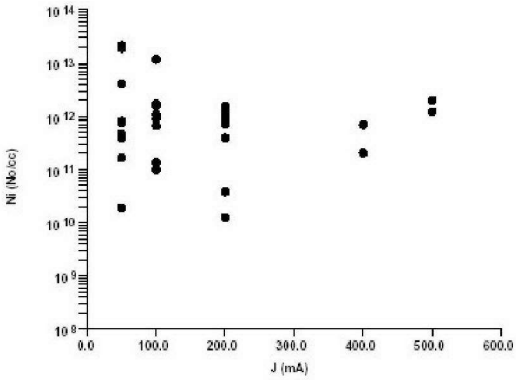

Figure 6 Ion number density of DC discharge

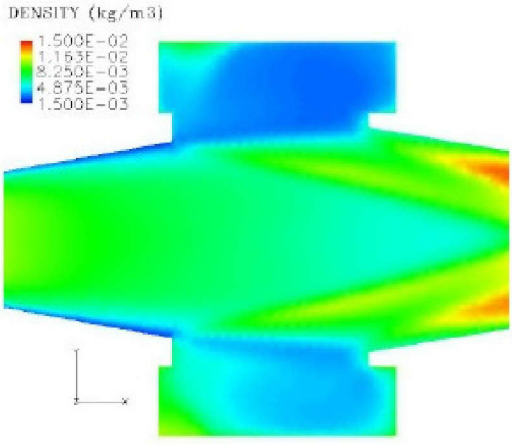

Figure 7 Closeup density contours in test section

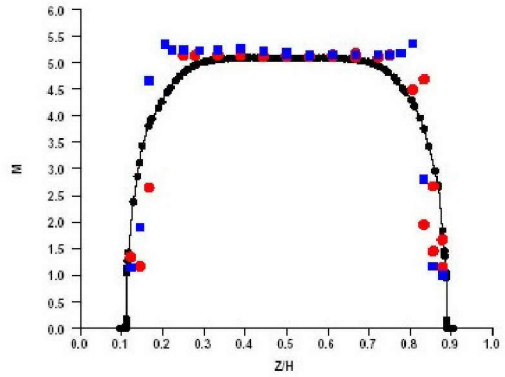

Figure 8 Vertical Mach number survey at the nozzle exit plane

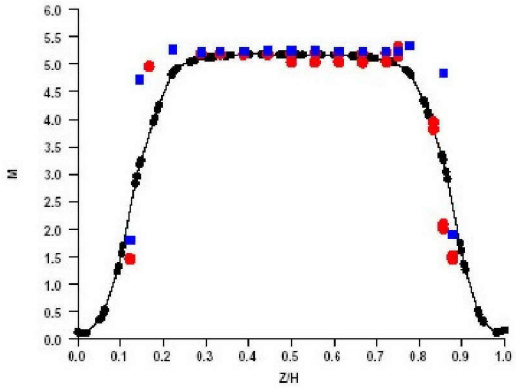

Figure 9 Vertical Mach number survey at 50.8 mm downstream

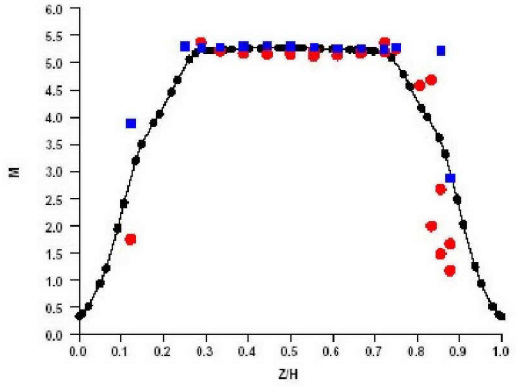

Figure 10 Vertical Mach number survey at 101.6 mm downstream

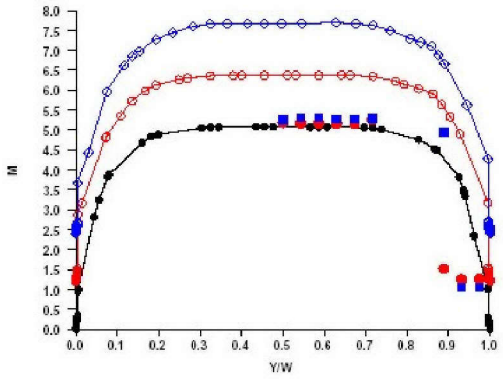

Figure 11 Transverse Mach number survey

---

[i] Resler, E. L., Jr., and Sears, W. R., "The Prospects for Magneto-Aerodynamics," *Journal of the Aeronautical Sciences*, vol. 25, no. 4, April 1958, pp. 235-245, 258.

[ii] Howatson, A. M., *An Introduction to Gas Discharges*, Pergamon Press, New York, 1976.

[iii] Roth, J. R., Sherman, D. M., and Wilkison, S. P., "Electrohydrodynamic Flow Control with a Glow-Discharge Surface Plasma," *AIAA Journal*, vol. 38,no. 7, July 2000, pp. 1166-1172.

[iv] Shang, J. S., Ganguly, B., Umstattd, R., Hayes, J., Arman, M., and Bletzinger, P., "Developing a Facility for Magneto-Aerodynamics Experiments, *Journal of Aircraft*, vol. 17, no. 7, Nov.-Dec., 2000, pp. 1065-1072.

[v] Miles, R. B., "Flow Control by Energy Addition into High-Speed Air, AIAA paper 2000-2324, June 2000.

[vi] White, A. R., Palm, P., Plonjes, E., Subramaniam, V. V., Adamovich, I. V., "Effect of Electron Density on Shock Wave Propagation in Optically Pumped Plasma," AIAA 2001-3058, June 2001.

[vii] Kimmel, R. L., Hayes, J. R., Shang, J. S., Lee, J., "Mach 5 Plasma Tunnel Update," Abstract presented at 27th Annual Dayton-Cincinnati Aerospace Science Symposium," March 2002.

[viii] Shang, J. S., Hayes, J., Harris, S., Umstattd, R., and Ganguly, B., "Experimental Simulation of Magneto-Aerodynamic Hypersonics, AIAA 2000-2258, June 2000.

[ix] Herzberg, G., Molecular Spectra and Molecular Structure, 1, Spectra of Diatomic Molecules, van Nostrand, New York, 1950, pp. 127-253.

[x] Menart, J., Shang, J., and Hayes, J., "Development of a Langmuir Probe for Plasma Diagnostic Work in High Speed Flow," AIAA paper 2001-2804, June 2001.

[xi] Plonjes, E., Palm, Pl, Adamovich, I. V., and Rich, J. W., "Characteristic of Electron-Mediated Vibration Electronic (V-E) Energy Transfer in Optically Pumped Plasma Using Langmuir Probe Measurements," AIAA paper 2002-2243, May 2002.

[xii] Menart, J. A., Shang, J., "Data Reduction Analysis for Cylindrical, Double Langmuir Probes Operating in Collisionless to Collisional, Quiescent Plasma," AIAA paper 2003-0136, January 2003.

[xiii] Menart, J. A., Shang, J. S., Henderson, S., Kurpik, A., Kimmel, R., and Hayes, J., "Survey of Plasmas Generated in a Mach 5 Wind Tunnel," AIAA paper 2003-1194, January 2003.

[xiv] Heald, M. A., and Wharton, C. B., *Plasma Diagnostic with Microwaves*, John Wiley & Son, New York, 1965.

[xv] Strang, W. Z., Tomaro, R. F., and Grismer, M., "The Defining Methods of $Cobat_{60}$: A Parallel, Implicit, Unstructured Euler / Navier-Stokes Flow Solver," AIAA 99-0786, January 1999.

[xvi] Gottleib, J. J., aand Groth, C. P. T., "Assessment of Riemann Solvers for Unsteady One-dimensional Inviscid Flows of Perfect Gases," *Jour. Comp. Physics*, vol. 78, no. 2, 1988, pp. 437-458.

[xvii] Grismer, M. J., Strang, W. Z., Tomaro, R. F., and Witzeman, F. C., "Cobalt: A Parallel, Implicit, Unstructured Euler / Navier-Stokes Solver," *Advances in Engineering Software*, vol. 29, April-July, 1998, pp. 365-373.